

Probing new gauge-boson couplings via three-body decays

J. L. Hewett and T. G. Rizzo

High Energy Physics Division, Argonne National Laboratory, Argonne, Illinois 60439

(Received 2 September 1992; revised manuscript received 15 December 1992)

We examine the possibility of using rare, three-body decays of a new neutral gauge boson Z_2 to probe its gauge couplings at hadron colliders. Specifically, we study the decays $Z_2 \rightarrow Wl\nu$ and $Z_2 \rightarrow Z\nu\bar{\nu}$ and find that much knowledge of the Z_2 properties can be obtained from these processes. In particular, these decay modes can yield valuable information on the amount of Z_1 - Z_2 mixing, on the generation dependence of the Z_2 couplings, and on the properties of the new generator associated with the Z_2 , as well as being used to distinguish between possible extended models. Standard model backgrounds to these three-body decays are discussed, and we find that the rate for $pp \rightarrow ZZ \rightarrow Z\nu\bar{\nu}$ eclipses that of $pp \rightarrow Z_2 \rightarrow Z\nu\bar{\nu}$ at hadron supercolliders. The analogous three-body decays into a new, heavy charged gauge boson, $Z_2 \rightarrow W_2^\pm l^\mp \nu$, are also investigated in models where this can occur.

PACS number(s): 13.38.+c, 12.15.Cc

It is now commonly accepted that if a new neutral gauge boson (Z') exists, it should be observed by direct production, via $pp \rightarrow Z' \rightarrow l^+l^-$, at both the Superconducting Super Collider (SSC) and CERN Large Hadron Collider (LHC) if its mass is of order a few TeV or less [1] (provided it couples to both $q\bar{q}$ and l^+l^- pairs at or near electroweak strength). Indeed, if a Z' is discovered we will want to learn as much about it as possible; in particular, the next logical step would be to determine its gauge couplings and the extended model from which it originates. Unlike e^+e^- machines, hadron colliders are limited to only a few measurable quantities with which the new gauge boson properties can be determined. In addition to obtaining the Z' mass, the planned SSC and LHC detectors [2] will be able to collect data on the Z' production cross section and subsequent decay into l^+l^- , the full Z' width, and the leptonic forward-backward asymmetry. Unfortunately, these measurements will not only be statistics limited but also will experience reasonably large systematic effects due to finite mass resolution and efficiencies as well as uncertainties in the collider luminosity. To further extract coupling information, uncertainties in the parton distributions will also contribute to the systematic errors. If, however, several theoretical assumptions are made, one can use the above data to distinguish new Z' bosons from different models with reasonable reliability [3].

In order to obtain more information on Z' couplings, we need an additional set of quantities, which do not suffer the large theoretical or systematic uncertainties discussed above, can be measured with reasonable statistics, and yet are sensitive to the particular extended model. Since decay modes involving leptons provide the cleanest signatures and the conventional l^+l^- mode is already being used to discover the Z' , one of the next possibilities to consider is various three-body decays. One potential process [4], which has recently been revived in the literature [5], is to look for the decay $Z' \rightarrow W^\pm l^\mp \nu$, and, in particular, to measure the ratio

$$r_{l\nu W} = \frac{\Gamma(Z' \rightarrow W^\pm l^\mp \nu)}{\Gamma(Z' \rightarrow l^+l^-)}, \quad (1)$$

which suffers very little from the above-mentioned systematic uncertainties. (We note that in this definition of $r_{l\nu W}$ we sum over both W^\pm modes, but there is no sum over l which we assume to be either e or μ .) A second such useful quantity [5] is the corresponding ratio

$$r_{\nu\nu Z} = \frac{\Gamma(Z' \rightarrow Z\nu_l\bar{\nu}_l)}{\Gamma(Z' \rightarrow l^+l^-)}, \quad (2)$$

wherein a sum over the three generations of $\nu_l\bar{\nu}_l$ is assumed. If one allows for decays of the Z' into two jets plus a W^\pm or Z , two additional quantities can be defined which parallel $r_{l\nu W}$ and $r_{\nu\nu Z}$ above. We feel, however, that though W^\pm or Z +jets final states from Z' decay might be separable from standard model (SM) backgrounds, these modes will not be clean. We then restrict our attention to $r_{l\nu W}$ and $r_{\nu\nu Z}$, where we will find that these two quantities have the potential to reveal much about the nature of the Z' . However, as we will see below, large SM backgrounds make the signal for $r_{\nu\nu Z}$ extremely difficult to observe.

We first examine the process $Z' \rightarrow W^\pm l^\mp \nu$ and the ratio $r_{l\nu W}$. In general, as discussed in Ref. [4], this reaction can proceed either by W emission off of a fermion leg, or via a $Z'W^+W^-$ coupling which exists only if the Z' mixes with the SM Z . The Feynman diagrams responsible for these contributions are displayed in Fig. 1. If Z - Z' mixing is nonvanishing, then both the Z and Z' are not mass eigenstates. The physical states will then be

$$\begin{aligned} Z_2 &= Z' \cos\phi - Z \sin\phi, \\ Z_1 &= Z' \sin\phi + Z \cos\phi, \end{aligned} \quad (3)$$

with the state Z_1 being the one probed at the CERN e^+e^- collider LEP, and $Z'(Z)$ must be replaced by $Z_2(Z_1)$ in the discussion above. We emphasize that the

$Z_2 W^+ W^-$ coupling only occurs via this mixing. Following Ref. [4] and Marciano and Wyler [6], we can then write the quantity $r_{l\nu W}$ as

$$r_{l\nu W} = \frac{G_F M_W^2}{2\sqrt{2}\pi^2} (v_{2l}^2 + a_{2l}^2)^{-1} \left\{ \frac{1}{2} [(v_{2l} + a_{2l})^2 + (v_{2\nu} + a_{2\nu})^2] H_1 + (v_{2l} + a_{2l})(v_{2\nu} + a_{2\nu}) H_3 \right. \\ \left. + \frac{1}{2} (-s_\phi c_W^2)^2 H_2 - s_\phi c_W^2 [(v_{2l} + a_{2l}) - (v_{2\nu} + a_{2\nu})] H_4 \right\}, \quad (4)$$

where the v 's and a 's represent the various vector and axial-vector couplings of the Z_2 to charged leptons and neutrinos, $s_\phi = \sin\phi$, and $c_W = \cos\theta_W$, with $x_W = \sin^2\theta_W$. Note that the last two terms in this expression are proportional to the amount of Z - Z' mixing and arise from the diagram of Fig. 1(c). The quantities H_i are the results of performing one-dimensional integrations over modified forms of the functions given in Ref. [6]. These modifications occur from $H_{2,4}$ only (the terms that arise from the $Z_2 W^+ W^-$ coupling), since we must now integrate over the W resonance requiring that the finite W width, Γ_W , be included in the calculation. This was not included in the analysis of Ref. [6] since both of the W 's could not be on shell simultaneously as $M_{Z_2} < 2M_W$. Thus the H_i functions depend only on M_{Z_2} , Γ_W , and the Z_2

mass, M_{Z_2} . Clearly, $r_{l\nu W}$ will be quite sensitive to $s_\phi \neq 0$; when $s_\phi = 0$, only the above terms with $H_{1,3}$ will remain. *For the moment*, we will assume that $s_\phi = 0$, and will neglect any possible influence from W - W' mixing. In Fig. 2 we present the number of events expected per year at the SSC with an integrated luminosity of 10^4 pb^{-1} from the process $pp \rightarrow Z_2 \rightarrow W^\pm l^\mp \nu$ as a function of the Z_2 mass for various extended models, which are discussed below. We see that hundreds of events are expected for Z_2 masses up to $\sim 2 \text{ TeV}$ in most models. Here we have included a lepton identification efficiency [2] of $\epsilon = 85\%$ for each lepton.

If a Z_2 exists, it must couple to a new diagonal generator D originating from an extended gauge group. If D and the ordinary $SU(2)_L$ generator T_{iL} commute, i.e., $[D, T_{iL}] = 0$, or if only

$$[D, T_{iL}] | \nu_L, l_L \rangle = 0 \quad (5)$$

is satisfied, then $v_{2l} + a_{2l} = v_{2\nu} + a_{2\nu}$ and $r_{l\nu W}$ simplifies to

$$r_{l\nu W} = \frac{G_F M_W^2}{2\sqrt{2}\pi^2} (H_1 + H_3) (v_{2l} + a_{2l})^2 (v_{2l}^2 + a_{2l}^2)^{-1}. \quad (4')$$

Note that Eq. (4') can never be satisfied when $s_\phi \neq 0$ since D will then contain the term $-s_\phi (T_{3L} - x_W Q)$ and neither Q nor T_{3L} commutes with $T_{1,2L}$. We will return to Eqs. (4) and (5) after a brief discussion of $r_{\nu\nu Z}$.

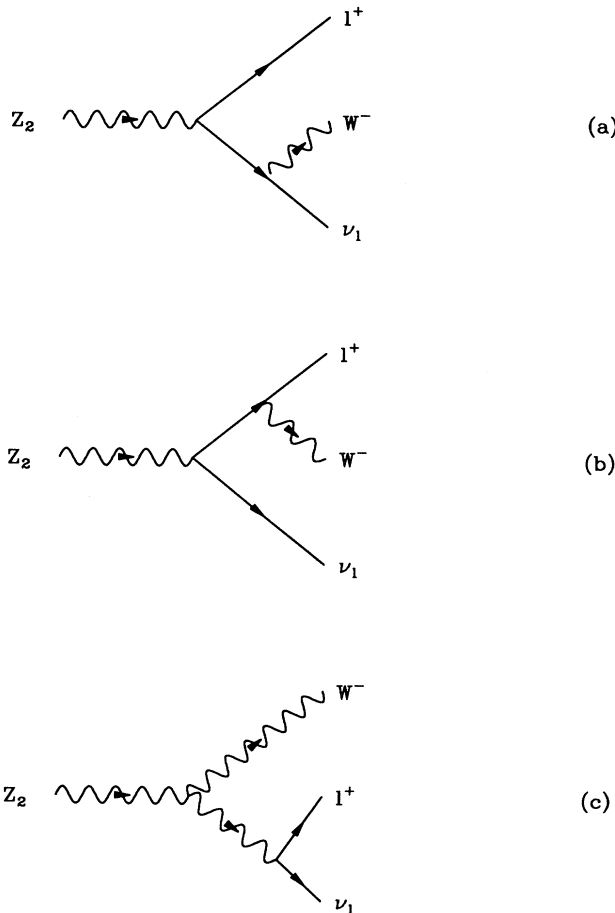


FIG. 1. Feynman diagrams responsible for the decay $Z_2 \rightarrow l\nu W$.

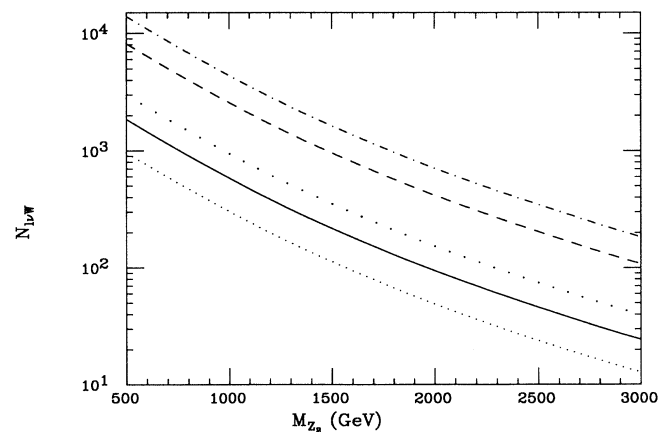


FIG. 2. Number of events expected for the process $Z_2 \rightarrow l\nu W$ neglecting Z - Z' mixing at the SSC with 10^4 pb^{-1} of integrated luminosity as a function of the Z_2 mass. From top to bottom, the dash-dotted curve corresponds to the SSM, the dashed curve to the HARV model (with $s_\chi = 0.5$), the dotted curve to the ALRM, the solid curve to the ER5M χ , and the short-dotted curve to the LRM.

Let us also examine the ratio

$$r \equiv \Gamma(Z_2 \rightarrow Z_1 f \bar{f}) / \Gamma(Z_2 \rightarrow l^+ l^-),$$

which is given by

$$r = \frac{G_F M_Z^2}{8\sqrt{2}\pi^2} N_c N_f \frac{(v_{1f} + a_{1f})^2 (v_{2f} + a_{2f})^2 + (v_{1f} - a_{1f})^2 (v_{2f} - a_{2f})^2}{v_{2l}^2 + a_{2l}^2} I, \quad (6)$$

where N_c is the usual color factor, I is a two-dimensional parameter integral which depends only on M_1^2/M_2^2 (when fermion masses are neglected), and N_f labels the number of flavors of a given type. For three generations of left-handed neutrinos, $N_c = 1$, $N_f = 3$, $v_{1\nu} = a_{1\nu}$, and $v_{2\nu} = a_{2\nu}$, so that

$$r_{\nu\nu Z} = \frac{3G_F M_Z^2}{2\sqrt{2}\pi^2} \frac{4v_{1\nu}^2 v_{2\nu}^2}{v_{2l}^2 + a_{2l}^2} I. \quad (7)$$

Here we have assumed that all the various couplings are generation independent in performing the sum over ν_e , ν_μ , and ν_τ . Note that with our normalization convention, $4v_{1\nu}^2 = 1$ when $s_\phi = 0$. We anticipate that, unlike $r_{l\nu W}$, $r_{\nu\nu Z}$ will not be greatly affected by $s_\phi \neq 0$; we will see further below that this is the case. For now, we continue to assume that $s_\phi = 0$ and also take Eq. (4') to be valid; we then see that

$$r_{\nu\nu Z} = K_Z \frac{v_{2\nu}^2}{v_{2l}^2 + a_{2l}^2}, \quad (8)$$

and, using the fact that $v_{2\nu} + a_{2\nu} = v_{2l} + a_{2l}$ together with $a_{2\nu} = v_{2\nu}$ we find

$$r_{l\nu W} = K_W \frac{v_{2\nu}^2}{v_{2l}^2 + a_{2l}^2}. \quad (9)$$

Here $K_{W,Z}$ are functions of the gauge boson masses only (M_2 , M_W , and M_1) and are *independent* of the choice of extended electroweak model. Thus, if the above conditions hold, all predictions for $r_{\nu\nu Z}/r_{l\nu W}$ must lie on a straight line, i.e.,

$$\frac{r_{\nu\nu Z}}{r_{l\nu W}} = \frac{K_Z}{K_W}. \quad (10)$$

Furthermore, Eqs. (8) and (9) tell us that *both* $r_{\nu\nu Z}$ and $r_{l\nu W}$ are bounded:

$$\begin{aligned} 0 \leq r_{l\nu W} &\leq \frac{1}{2} K_W, \\ 0 \leq r_{\nu\nu Z} &\leq \frac{1}{2} K_Z, \end{aligned} \quad (11)$$

with the lower (upper) end points of these ranges occurring for a purely right-handed (left-handed) Z_2 coupling to leptons. Thus not only is the ratio $r_{\nu\nu Z}/r_{l\nu W}$ model independent, but the value of the quantities themselves are restricted to a small region of the $r_{\nu\nu Z}$ - $r_{l\nu W}$ plane, with both being dictated *solely* by the values of $M_{1,2}$ and M_W . In addition, the position of the measured values of $r_{\nu\nu Z}$ and $r_{l\nu W}$ along the line will yield information on the ratio of the vector and axial-vector couplings of the Z_2 , up to a

twofold ambiguity, $v_l \leftrightarrow a_l$.

As an application of these results, we now examine the $r_{\nu\nu Z}$ - $r_{l\nu W}$ plane for some of the more well-known extended gauge models, taking $M_2 = 1$ TeV for purposes of demonstration. We also use $M_1 = 91.175$ GeV, $M_W = 80.14$ GeV, $\Gamma_W = 2.15$ GeV [7] and $x_W = 0.2330$ in our numerical analysis below. We stress that all these results assume $s_\phi = 0$.

Most extended models have generation independent couplings and have generators satisfying Eq. (5), thus predicting that the set of values for $r_{\nu\nu Z}$ versus $r_{l\nu W}$ lie on a bounded line segment; this is seen explicitly in Fig. 3. The solid line indicates the range of values permitted in the superstring-inspired E_6 effective rank-5 model ER5M [8], where the Z_2 couplings depend upon a parameter $-\theta \leq \theta \leq \theta$. In the figure, ψ labels the point $\theta = 0^\circ$, whereas χ labels the point $\theta = \pm 90^\circ$ in these models. In the left-right-symmetric model (LRM) [9] the only free parameter is the ratio of the $SU(2)_{L,R}$ couplings, $\kappa = g_R/g_L$ [10]. Note that on general grounds, it is expected [11] that $\kappa \leq 1$. L labels the point in the figure where $g_R/g_L = 1$, while the extreme case of $\kappa^2 = x_W(1-x_W)^{-1}$ coincides with the point χ . The position of the prediction for the alternative left-right model (ALRM) [12], based on E_6 theories, is labeled by A , and that of the Foot-Hernández (FH) model [13] is labeled by F . The expectations for the Z_2 model of Mahanthappa and Mohapatra [14], where the new generator D is proportional to $Y/2$, coincides with those of FH. Although all these models are quite different, their predictions for

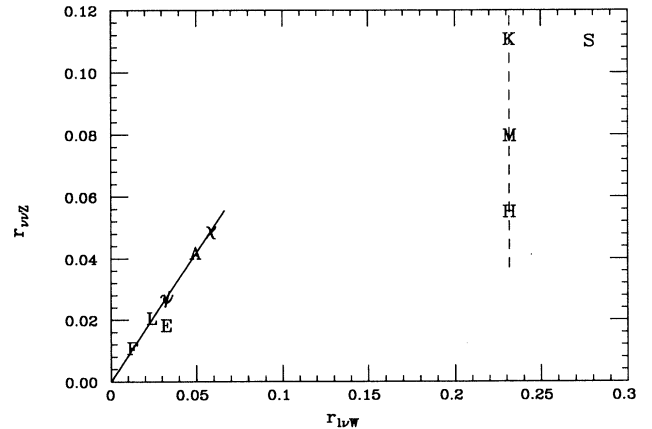


FIG. 3. Values of $r_{\nu\nu Z}$ and $r_{l\nu W}$ predicted by the various models discussed in the text when $s_\phi = 0$.

the ratio $r_{\nu\nu Z}/r_{l\nu W}$ are found to lie on a straight line within the bounded region as expected.

Other models shown in Fig. 3 demonstrate how Eqs. (10) and (11) can be violated if certain conditions are met. Several models predict that the new generator, D , will not satisfy Eq. (5), particularly if the Z_2 couplings are proportional to T_{3L} . In the ununified model (HARV) of Georgi *et al.* [15] (labeled by H in the figure), $D \sim t_\chi T_{3L}^l - T_{3L}^q t_\chi^{-1}$, where $t_\chi = \tan\chi$ with χ being a mixing parameter, and $T_{3L}^{l,q}$ are the third components of the lepton and quark isospin generators. Clearly, Eq. (5) and thus Eqs. (10) and (11) are not satisfied in this case. This can also happen in some compositeness-based Z_2 models [16], or ones which predict that the Z_2 is just a heavier version [17] of the Z_1 ; in the latter case, the prediction is marked by S in the figure, while a Z_2 whose couplings directly depend on T_{3L}^l will occupy the same position on the figure as in the model of Georgi *et al.*

A second possible source of deviation from the straight line prediction of Eq. (10) arises from the additional assumption used in Eq. (7) that the leptonic couplings of the Z_2 are generation independent. In the model of Kuo and collaborators [18] (KUO), the third generation couples differently than the first two, whereas, in the Leptophilic model [19], where differences in lepton number are gauged, the third generation decouples completely from the Z_2 . The expected values of $r_{l\nu W}$ and $r_{\nu\nu Z}$ in these two models are labeled by K and E , respectively, in Fig. 3. In the Leptophilic case, the values shown in the figure are only for purposes of demonstration, since this Z_2 cannot be produced at a hadron collider. As a last example, the predictions from the model of Li and Ma [20], which also results in a violation of universality, are found to lie along the vertical dashed curve labeled by m with the particular position being dependent upon the value of a model parameter p . For $p = \frac{1}{3}$, the model of Kuo *et al.* is recovered. In fact, one finds that the expectations in all models with generation dependent couplings and with $D \sim T_{3L}^l$ lie along this dashed line in Fig. 3. None of these models will generate values of $r_{\nu\nu Z}$ and $r_{l\nu W}$ which lie on the straight solid line predicted in Eq. (10).

To summarize our results so far, we have observed that if the following conditions hold:

- (i) $s_\phi = 0$,
- (ii) $[D, T_{iL}]|_{\nu_L, l_L} > 0$,
- (iii) v_{2f} and a_{2f} are generation independent,

then and only then will $r_{\nu\nu Z}/r_{l\nu W}$ be model independent and both quantities be separately bounded by $\frac{1}{2}K_{W,Z}$. Thus, if a Z_2 is discovered and its corresponding values of $r_{\nu\nu Z}$ and $r_{l\nu W}$ are determined, and it is observed that these values lie “elsewhere” on the $r_{\nu\nu Z}$ - $r_{l\nu W}$ plane rather than along the solid line, one can safely conclude that at least one of the above conditions (i)–(iii) are not valid. We have seen, however, that for $s_\phi = 0$ only rather “exotic” extended models, which do not arise from conventional grand unified theories, fail to satisfy these conditions.

As a final point of this discussion, we stress that a mea-

surement of $r_{l\nu W}$ and $r_{\nu\nu Z}$ alone cannot uniquely determine the model of origin of the Z_2 . This can be seen clearly from Fig. 3, e.g., in the case where the LRM and a particular value of θ from the ER5M predict the same pair of values for $r_{l\nu W}$ and $r_{\nu\nu Z}$. Even within the ER5M itself, except for the cases where $r_{\nu\nu Z} = r_{l\nu W} = 0$ and $r_{\nu\nu Z} = \frac{1}{2}K_Z$, $r_{l\nu W} = \frac{1}{2}K_W$ (i.e., the two end points of the line), each point along the line corresponds to two distinct values of the θ parameter resulting from the $\nu_l \leftrightarrow a_l$ ambiguity mentioned above. Thus, other data will be required to uniquely determine the origin of the Z_2 . We note that the leptonic forward-backward asymmetry (in the narrow width approximation) at hadron colliders is also invariant when the vector and axial-vector couplings of the Z_2 are flipped for both quarks and leptons. We also mention in passing that, as discussed in Ref. [5], not much information can be gained by considering the ratio r_{llZ} ($\equiv r$ in Eq. (6) with $f=l$). In this case we find

$$\begin{aligned} r_{llZ} &= K'_Z \left[1 + \left[\frac{2v_{1l}a_{1l}}{v_{1l}^2 + a_{1l}^2} \right] \left[\frac{2v_{2l}a_{2l}}{v_{2l}^2 + a_{2l}^2} \right] \right] \\ &= K'_Z \left[1 + 0.135 \left[\frac{2v_{2l}a_{2l}}{v_{2l}^2 + a_{2l}^2} \right] \right], \end{aligned} \quad (13)$$

where K'_Z is again a model-independent constant and the last equality holds for $s_\phi = 0$ and $x_W = 0.2330$. The sensitivity to coupling variations in r_{llZ} is thus seen to be substantially reduced compared to both $r_{l\nu W}$ and $r_{\nu\nu Z}$.

Next we examine what happens when a Z_2 , which satisfies conditions (ii) and (iii) above when $s_\phi = 0$, is now allowed to mix with the SM Z , i.e., what happens when s_ϕ is nonzero. Clearly, condition (iii) remains valid, but if (i) is violated so is (ii), as the new generator D now has a term proportional to $s_\phi T_{3L}$. For the case of $r_{l\nu W}$, both terms H_2 and H_4 in Eq. (4) will now contribute. To be specific, we examine the effect of $s_\phi \neq 0$ in the ER5M, ALRM, and LRM (with $\kappa = 1$); all of which satisfy conditions (ii) and (iii) when $s_\phi = 0$. We first summarize some properties of the Z - Z' mixing mechanisms before discussing its effect on $r_{l\nu W}$ and $r_{\nu\nu Z}$.

For an extended model with Higgs scalars transforming only as $SU(2)_L$ doublets or singlets, the Z - Z' mass matrix can be written as

$$\begin{pmatrix} M_Z^2 & \gamma M_Z^2 \\ \gamma M_Z^2 & M_Z^2 \end{pmatrix}, \quad (14)$$

with γ being a model dependent parameter of order unity and M_Z the value of the SM Z -boson mass in the absence of mixing. The eigenvalues of this matrix, $M_{1,2}^2$, correspond to the masses of the physical gauge bosons $Z_{1,2}$ given in Eq. (3). Since M_1 is known from LEP [21] ($=91.175$ GeV), the value of ϕ is calculable from the above Eq. (14), for a given value of the Z_2 mass, M_2 , in a particular model (which then determines γ). We can write

$$M_Z^2 = \frac{M_1^2 + M_2^2 - [(M_2^2 - M_1^2)^2 - 4\gamma^2 M_1^2 M_2^2]^{1/2}}{2(1 + \gamma^2)}, \quad (15)$$

$$M_Z^2 = M_1^2 + M_2^2 - M_Z^2,$$

so that one obtains

$$\phi(M_2, \gamma) = \frac{1}{2} \arctan \left[\frac{2\gamma M_Z^2}{M_Z^2 - M_Z^2} \right]. \quad (16)$$

For the various models we consider, γ is given by

$$\gamma_{\text{LRM}} = -(1 - 2x_W)^{1/2},$$

$$\gamma_{\text{ALRM}} = \frac{x_W t_\beta^2 - (1 - 2x_W)}{(1 - 2x_W)^{1/2}(1 + t_\beta^2)}, \quad (17)$$

$$\gamma_{\text{ER5M}} = -2 \left[\frac{5x_W}{3} \right]^{1/2} \left[\left[\frac{c_\theta}{\sqrt{6}} - \frac{s_\theta}{\sqrt{10}} \right] t_\beta^2 - \left[\frac{c_\theta}{\sqrt{6}} + \frac{s_\theta}{\sqrt{10}} \right] \right] (1 + t_\beta^2)^{-1},$$

where $t_\beta = \tan\beta = v_t/v_b$, the usual ratio of vacuum expectation values (VEV's) responsible for the top and bottom quark masses, and $s_\theta(c_\theta) = \sin\theta(\cos\theta)$ being the ER5M mixing angle discussed above. Note that if $\theta = -90^\circ$ (model χ) then $\gamma_\chi = -(2x_W/3)^{1/2}$ is independent of the value of $\tan\beta$. In obtaining these expressions, we have made the following assumptions. For the ER5M and ALRM which are based on superstring-inspired E_6 , we assume that the only scalars responsible for $SU(2)_L$ breaking are the SUSY partners of the exotic fermions N and N^c that lie in the 27 representation. Since the quantum numbers of these fields are fixed (for a given value of θ in the ER5M case), this completely determines γ except for the VEV ratio, $\tan\beta$. In the LRM case, assuming that the left-handed triplet VEV is small implies that the fields in the ‘‘mixed-doublet’’ representation, $(\frac{1}{2}, \frac{1}{2})$ of $SU(2)_L \times SU(2)_R$ are mainly responsible for $SU(2)_L$ breaking. In this case, the $\tan\beta$ dependence factors out and one is left with the above expression. We have for the moment also ignored the possible influence of W - W' mixing in the LRM case.

Since γ is independent of $\tan\beta$ in both model χ and the LRM, the value of s_ϕ is then uniquely determined in these cases once M_2 is specified. Figures 4(a) and 4(b) display $r_{l\nu W}$ as a function of M_2 for (a) model χ and (b) the LRM with γ as given above (i.e., $s_\phi \neq 0$) and, for comparison, with $s_\phi = 0$ set by hand. Clearly the effects of $s_\phi \neq 0$ on $r_{l\nu W}$ are quite striking as it produces a very substantial increase in the value of this parameter. (This result was anticipated quite some time ago in Ref. [4].) Since γ is $\tan\beta$ dependent in the other models, we present $r_{l\nu W}$ as a function of $\tan\beta$ in Fig. 5(a), assuming $M_2 = 1$ TeV, for the ALRM and the three ER5M's corresponding to $\theta = 0^\circ$ (model ψ), $\theta = \arcsin \sqrt{\frac{3}{8}} \approx 37.76^\circ$ (model η), and $\theta = -\arcsin \sqrt{\frac{3}{8}} \approx -52.24^\circ$ (model I). In all cases, varying $\tan\beta$ away from the point where $\gamma = 0$, i.e., $\tan\beta = 1(2, \approx 1.5)$ for model ψ (model η , ALRM), which

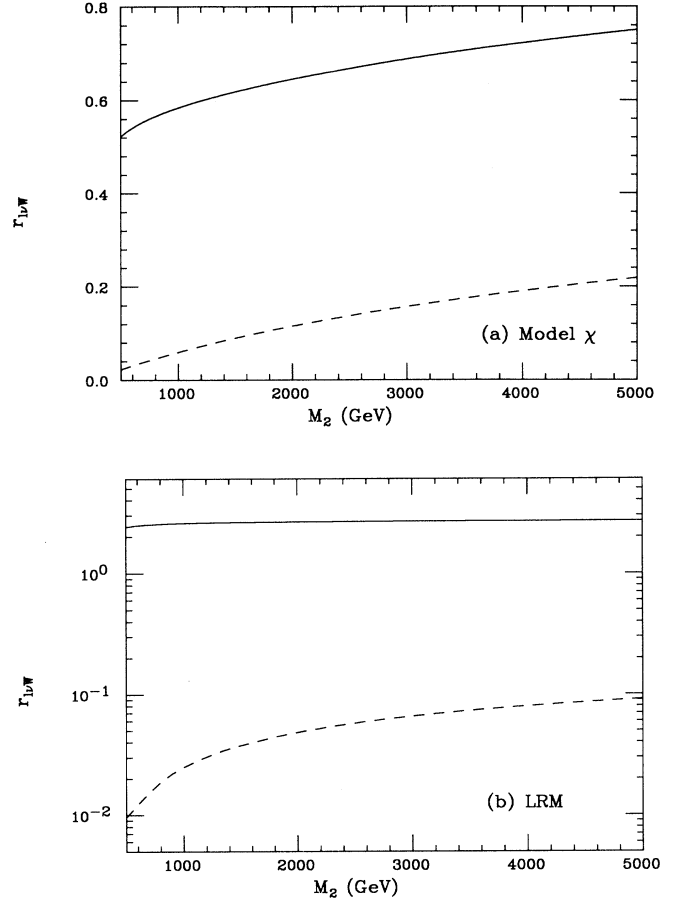


FIG. 4. A comparison of the predicted values of the ratio $r_{l\nu W}$ in (a) model χ and (b) the LRM as a function of M_2 both with (solid curve) and without (dashed curve) Z - Z' mixing.

corresponds to $s_\phi = 0$, can produce a substantial increase in the value of $r_{l\nu W}$. A minimal value of $r_{l\nu W}$, corresponding to a choice of $\tan\beta$ which produces $s_\phi = 0$, will exist for all values of θ in the range $-\sqrt{\frac{5}{3}} \leq \tan\theta \leq \sqrt{\frac{5}{3}}$. The value of $\tan\beta$ which yields these minima is given by

$$\tan^2\beta = \frac{1 + \sqrt{\frac{3}{5}}\tan\theta}{1 - \sqrt{\frac{3}{5}}\tan\theta}. \quad (18)$$

Thus, for example, model I, with $\tan\theta = -\sqrt{\frac{5}{3}}$, will not experience any true minima of $r_{l\nu W}$ for finite values of $\tan\beta$. This is demonstrated in Fig. 5(b), which is a three-dimensional plot of $r_{l\nu W}$ as a function of $\tan\beta$ and θ , where a minima ‘‘valley’’ is clearly observable. We conclude that even though $|\phi| \approx 10^{-3}$ for M_2 in the TeV range, this small amount of mixing can substantially modify the expectations for the value of $r_{l\nu W}$ within a given model.

How does Z - Z' mixing modify the values of $r_{\nu\nu Z}$? We anticipate that there is little effect since $s_\phi \neq 0$ does not induce a resonant contribution to this ratio. Hence, for this case, the inclusion of mixing only results in a slight

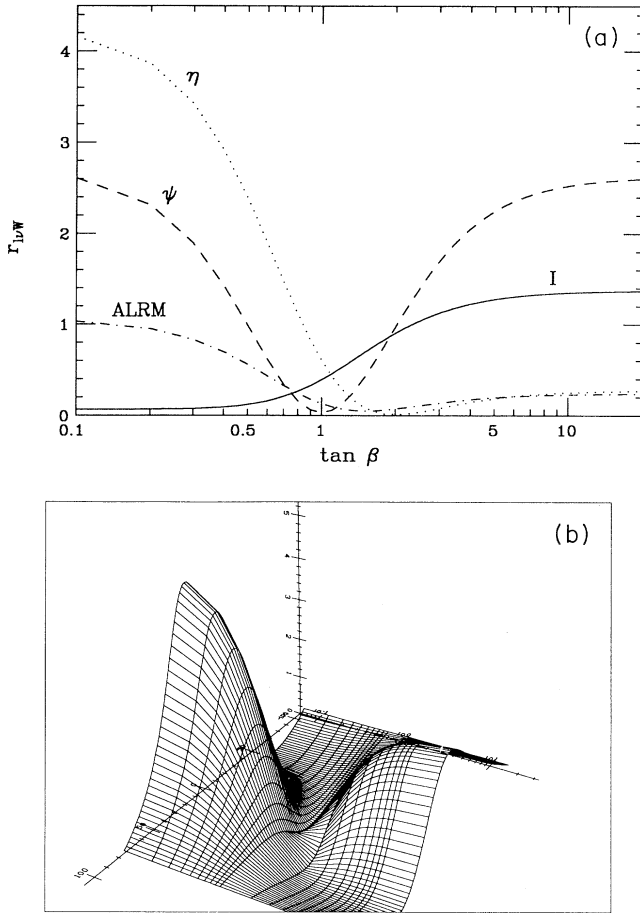


FIG. 5. (a) $r_{l\nu W}$ as a function of $\tan\beta$ assuming $M_2=1$ TeV for the E_6 ER5M I (corresponding to $\theta=-52.24^\circ$), represented by the solid curve; model η ($\theta=37.76^\circ$), dotted curve, and model ψ ($\theta=0^\circ$), dashed curve; as well as the ALRM, dash-dotted curve. (b) Three-dimensional figure of $r_{l\nu W}$ as a function of $\tan\beta$ and θ in the ER5M. The x axis corresponds to θ (ranging from -100° to $+100^\circ$), the y axis to $\tan\beta$ (ranging from 10^{-1} to 10^1), and the z axis to $r_{l\nu W}$ (ranging from 0 to 5).

shift of the gauge boson coupling constants. Figures 6(a) and 6(b) show $r_{\nu\nu Z}$ as a function of M_2 for (a) model χ and (b) the LRM, and demonstrate that our expectations are correct. Thus, for models which satisfy conditions (ii) and (iii) of Eq. (12) when $s_\phi=0$, the cleanest signal for $s_\phi\neq 0$ is that $r_{l\nu W}$ would be substantially increased while $r_{\nu\nu Z}$ would suffer only a slight modification. This would correspond to a shift of the model predictions to the right and off of the straight line in Figure 1. If $r_{\nu\nu Z}$ and $r_{l\nu W}$ were the only properties of the Z_2 that were measured, this would imply that it would be impossible to separate a model which violates conditions (ii) and (iii) with $s_\phi=0$ from a model which is shifted off of the straight line due to a nonzero value of s_ϕ . As an example, the Leptophilic model Z_2 would be indistinguishable from an ER5M Z_2 with $\theta\simeq 10^\circ$ and with a value of $\tan\beta$ which increases $r_{l\nu W}$ (via $s_\phi\neq 0$) by a small amount. However, the obser-

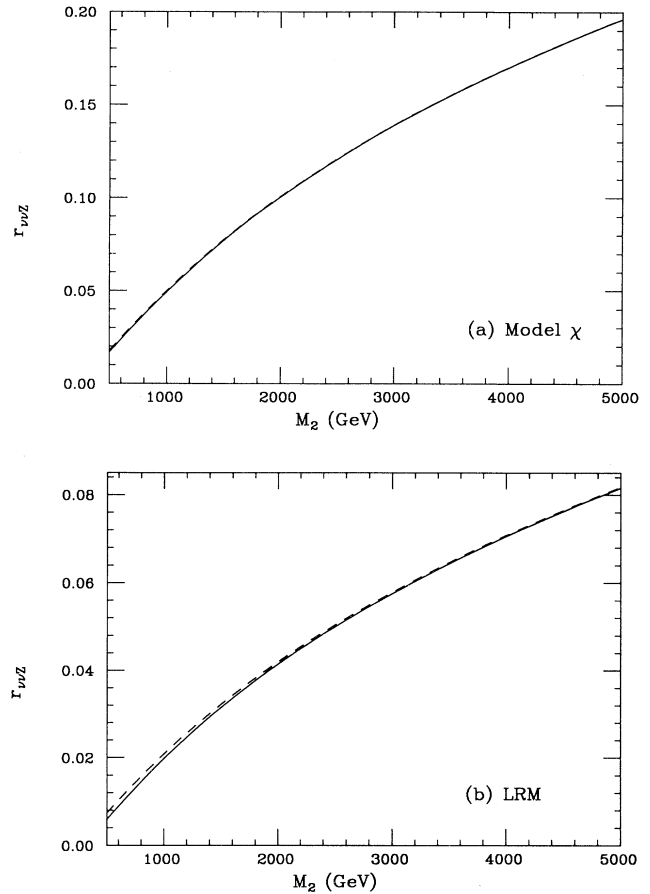


FIG. 6. Same as Fig. 4 but for the ratio $r_{\nu\nu Z}$.

vation of a violation of the bound on $r_{\nu\nu Z}$ in Eq. (11), would clearly signal that the conditions (ii) or (iii) are violated *independently* of whether or not $s_\phi=0$. Thus, while $r_{l\nu W}$ is the more sensitive probe for the validity of condition (i), the ratio $r_{\nu\nu Z}$ does the corresponding job of testing the validity of conditions (ii) and (iii). Combining knowledge of the values of $r_{l\nu W}$ and $r_{\nu\nu Z}$ with the measured values of the relative branching fractions for the processes $Z_2\rightarrow e^+e^-$, $\mu^+\mu^-$, and $\tau^+\tau^-$ would completely determine the validity of any of these conditions.

The greatest difficulty with using $r_{\nu\nu Z}$ as a probe of the Z_2 couplings arises from the large SM background from the process $pp\rightarrow 2Z\rightarrow Z\nu\bar{\nu}$. In order to compare the Z_2 signal to the SM background, we present the missing transverse momentum distributions for both processes at the SSC and LHC with rapidity (Y) cuts of 2.5 and 0.5 in Figs. 7(a) and 7(b), respectively, assuming a Z_2 mass of 1 TeV. The SM distributions fall rapidly with increasing values of missing p_t due to the presence of t - and u -channel poles in the amplitude which force the two Z 's to appear at small angles while still carrying large energies in the parton-parton center-of-mass frame. On the other hand, the rather soft missing p_t distribution in the Z_2 case is instead due to the bremsstrahlung nature of the Z production process. In all cases, the missing p_t distribu-

tion shown for the $Z_2 \rightarrow Z\nu\bar{\nu}$ signal in these figures must be rescaled by a model- and rapidity-cut-dependent factor, f , which in the narrow width approximation is given by

$$f \equiv \left[\frac{\sigma B_l}{1 \text{ pb}} \right] \frac{v_{2\nu}^2}{v_{2l}^2 + a_{2l}^2}, \quad (19)$$

where σ is the Z_2 production cross section (after appropriate rapidity cuts) and B_l is the Z_2 leptonic branching fraction. Quite generally, one expects f to lie in the range 0.1–1 for most models depending on the rapidity cut and machine center-of-mass energy. Table I and Figs. 7(c)–7(e) display the quantity f for the SSC and LHC with both choices of the Y cut for a large number of

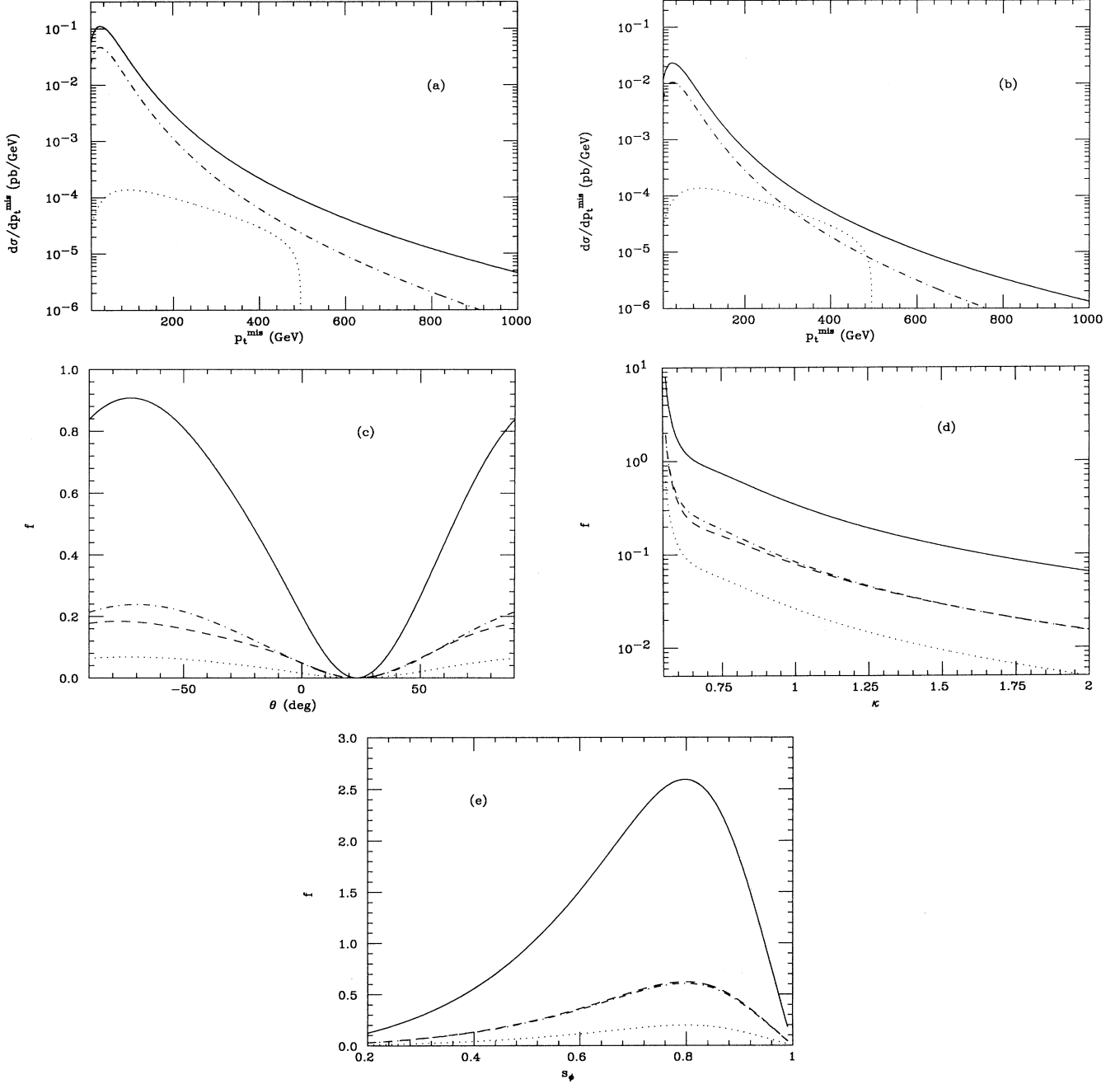


FIG. 7. Missing p_t distribution for the background process, $pp \rightarrow 2Z \rightarrow Z\nu\bar{\nu}$, at the SSC (solid) and LHC (dash-dotted) and for the signal, $pp \rightarrow Z_2 \rightarrow Z\nu\bar{\nu}$, assuming a rapidity cut of (a) 2.5 or (b) 0.5. The signal distribution must be scaled by the factor f described in the text. (c) Value of f as a function of the parameter θ in the ER5M at the SSC with a rapidity cut of 2.5 (solid) or 0.5 (dash-dotted) and at the LHC for a rapidity cut of 2.5 (dashed) or 0.5 (dotted). (d) Same as (c) but for the LRM as a function of the parameter κ . (e) Same as (c) but for the HARV model as a function of the parameter s_ϕ . In all cases, $M_2 = 1$ TeV is assumed.

TABLE I. Values of the parameter f for the SSC and LHC assuming either value for the rapidity cut for several different electroweak models discussed in the text.

Model	SSC		LHC	
	2.5	0.5	2.5	0.5
ALRM	1.172	0.249	0.314	0.091
SSM	2.794	0.664	0.656	0.213
LRM ($\kappa=1$)	0.344	0.083	0.079	0.026
KUO	1.118	0.261	0.268	0.085
ISO	2.236	0.523	0.536	0.171
ψ	0.202	0.047	0.048	0.015
χ	0.838	0.214	0.178	0.063
η	0.090	0.020	0.022	0.007
HARV ($s_\chi=0.5$)	0.955	0.223	0.229	0.073

extended electroweak models. Combining these results with those shown in Figs. 7(a) and 7(b) we see that the ratio of the signal to background is somewhat larger when the stronger rapidity cuts are made and missing p_i cuts are imposed. However, we also see that the signal always tends to lie a factor of 2–3 below the SM backgrounds for all values of missing p_i at both the SSC and LHC unless f takes on large values. A clean measurement of the ratio $r_{\nu\nu Z}$ appears hopeless, unless the background can be determined directly from experiment.

As mentioned above, one could also gain information [5] from the decays $Z_2 \rightarrow W + \text{jets}$ and $Z_2 \rightarrow Z + \text{jets}$, however these particular processes will also suffer from severe SM backgrounds, such as W or $Z + n$ -jet production. Not only is the leptonic process $Z_2 \rightarrow Wl\nu$ cleaner to begin with, but its kinematic distributions should be able to differentiate it from SM backgrounds such as $pp \rightarrow WW$, as well. The fermions in the decay $Z_2 \rightarrow f\bar{f}$ will come out relatively back to back and the gauge boson, which is radiated off of one of the fermion legs via bremsstrahlung, will be approximately collinear with the fermion and relatively soft. Also, the resonance graph, $Z_2 \rightarrow W^+W^-$ will have different kinematical properties [22].

Up to this point, we have ignored the possibility that a new charged gauge boson, W_2^\pm , may also participate in three-body Z_2 decays. New charged gauge bosons are present in several of the models discussed above, in particular, the LRM [9], ALRM [12], Li and Ma model [20], and HARV model [15]. In the Li and Ma and HARV cases, the Z_2 and W_2^\pm are essentially degenerate so that W_2^\pm final states in Z_2 decay are uninteresting. This is not generally the case for either the LRM or ALRM, where $Z_2 \rightarrow W_2^\pm l^\pm \nu_R$ is always kinematically accessible. The two-body decay $Z_2 \rightarrow W_2^+ W_2^-$ might also be allowed in the LRM for a certain range of the model parameters. To be concrete, we will neglect any effects associated with

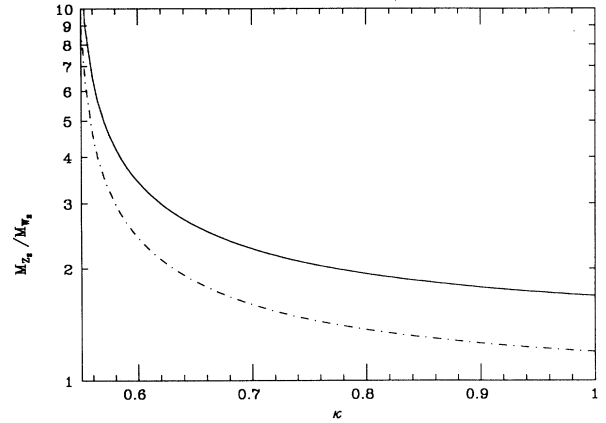


FIG. 8. The ratio M_{Z_2}/M_{W_2} as a function of κ for a triplet (solid curve) or doublet (dash-dotted curve) symmetry-breaking sector.

W - W' mixing (which is naturally absent in the ALRM) and Z - Z' mixing. The Z_2 to W_2^\pm mass ratio is

$$\frac{M_{Z_2}^2}{M_{W_2}^2} = \frac{\kappa^2(1-x_W)}{\kappa^2(1-x_W)-x_W} \rho_R, \quad (20)$$

where $\kappa \equiv g_R/g_L$ is the ratio of $SU(2)_{L,R}$ couplings, and ρ_R probes the symmetry-breaking sector relevant for the heavy gauge boson pair:

$$\rho_R \equiv \frac{2 \sum_i T_{3R_i}^2 v_i^2}{\sum_i [T_{R_i}(T_{R_i}+1) - T_{3T_i}^2] v_i^2} = \begin{cases} 1 & \text{Higgs doublets,} \\ 2 & \text{Higgs triplets.} \end{cases} \quad (21)$$

Here, the sum extends over the Higgs sector, v_i is the VEV of the i th Higgs boson, and $T_{R_i}(T_{3R_i})$ is the value of isospin (third component of isospin) of the neutral Higgs boson under $SU(2)_R$ [10]. In the LRM, $0.55 \lesssim \kappa \lesssim 1$ and ρ_R takes either value depending on whether the neutrinos are Majorana or Dirac particles, whereas in the ALRM, $\kappa = \rho_R = 1$ only. The two-body decay $Z_2 \rightarrow W_2^+ W_2^-$ is kinematically accessible in the LRM for the range $\kappa \lesssim 0.63(0.77)$ with a doublet (triplet) $SU(2)_R$ symmetry-breaking sector. Figure 8 displays the ratio M_{Z_2}/M_{W_2} as a function of κ for both Higgs doublet and triplet representations.

Denoting the $Z_2 W_2^+ W_2^-$ coupling as λg_R , we can define a ratio similar to $r_{l\nu W}$ above:

$$\begin{aligned} r_{l\nu W_R} &\equiv \frac{\Gamma(Z_2 \rightarrow W_2^\pm l \nu_R)}{\Gamma(Z_2 \rightarrow l^+ l^-)} \\ &= \frac{G_F M_W^2}{2\sqrt{2}\pi} (v_{2l}^2 + a_{2l}^2)^{-1} \left\{ \frac{1}{2} [(v_{2l} - a_{2l})^2 + (v_{2\nu_R} - a_{2\nu_R})^2] H'_1 + (v_{2l} - a_{2l})(v_{2\nu_R} - a_{2\nu_R}) H'_3 \right. \\ &\quad \left. + \frac{1}{2} \kappa^2 \lambda^2 H'_2 + \kappa \lambda [(v_{2l} - a_{2l}) - (v_{2\nu_R} - a_{2\nu_R})] H'_4 \right\}, \quad (22) \end{aligned}$$

where $H'_i = H_i$ with the replacements $M_W \rightarrow M_{W_2}$, $\Gamma_W \rightarrow \Gamma_{W_2}$. All four terms will contribute to $r_{l\nu W_R}$ since the couplings are always linearly proportional to T_{3R} (i.e., the condition $v_{2l} - a_{2l} = v_{2\nu_R} - a_{2\nu_R}$ does not hold in the LRM or the ALRM). The parameter λ introduced above is given by

$$\lambda = \left[\frac{\kappa^2 - (1 + \kappa^2)x_W}{\kappa^2(1 - x_W)} \right]^{1/2}, \quad (23)$$

which is simply M_{W_2}/M_{Z_2} for $\rho_R = 1$ (in analogy with the factor $c_W = M_W/M_Z$ which is present in the SM trilinear coupling). We note that the expression for $r_{l\nu W_R}$ assumes that ν_R is light relative to the Z_2 and W_2^\pm ; this is an excellent approximation in the LRM with a doublet Higgs representation and in the ALRM where ν_R is expected to be light (the exotic fermion S_L^c in the **27** representation of E_6 , Ref. [8], plays the role of the right-handed neutrino in the ALRM). For completeness, we note that the rate for Z_2 decay to an *on-shell* pair of W_2 's is given by

$$\Gamma(Z_2 \rightarrow W_2^+ W_2^-) = \frac{G_F M_W^2}{24\sqrt{2}\pi} M_{Z_2} \lambda^2 \kappa^2 \left[\frac{M_{Z_2}^2}{M_{W_2}^2} \right]^2 \left[1 - \frac{4M_{W_2}^2}{M_{Z_2}^2} \right]^{3/2} \left\{ 1 + 20 \left[\frac{M_{W_2}^2}{M_{Z_2}^2} \right] + 12 \left[\frac{M_{W_2}^2}{M_{Z_2}^2} \right]^2 \right\}. \quad (24)$$

This width is potentially large for smaller values of κ , as in this case $M_{Z_2}^2 \gg M_{W_2}^2$ and no mixing angle suppression appears. Figure 9 presents the reduced width $\Gamma_R \equiv \Gamma(Z_2 \rightarrow W_2^+ W_2^-)/M_{Z_2}$ as a function of κ for both types of symmetry-breaking sectors; note that in order to set the scale and guide the eye, the corresponding ratio for the SM Z decay into e^+e^- is $\simeq 9.1 \times 10^{-4}$. We see from the figure that Γ_R is only significant for the double Higgs representation when $\kappa \lesssim 0.61$, but remains much larger in the triplet case out to values of $\kappa \simeq 0.73$.

Figure 10 shows the ratio $r_{l\nu W_R}$ as a function of κ for both the triplet and doublet symmetry-breaking schemes assuming $M_{Z_2} = 4$ TeV for purposes of demonstration. (This choice of M_{Z_2} was made in order to avoid too light a value of M_{W_2} for small κ .) In the Higgs triplet case, $r_{l\nu W_R}$ remains above 10^{-2} for almost all the entire range of κ , whereas, the ratio drops below this value for $\kappa \simeq 0.63$ in the case of scalar doublets. The very large value of $r_{l\nu W_R}$ at small κ values arises from the strong resonant

contribution, $Z_2 \rightarrow W_2^+ W_2^-$, in a manner similar to what we saw above in the case of Z - Z' mixing for $Z_2 \rightarrow W_1^+ W_1^-$. Similar results are obtainable for other values of M_{Z_2} . For the ALRM, where $\kappa = \rho_R = 1$, $r_{l\nu W_R}$ is found to be extremely small and unobservable, i.e., $\lesssim 10^{-4}$.

In summary, we have examined the three-body decays, $Z_2 \rightarrow Wl\nu$ and $Z_2 \rightarrow Z\nu\bar{\nu}$, and have found that they can be used to obtain much information on the properties of the Z_2 for $M_{Z_2} \lesssim 2-3$ TeV. In addition to being used to differentiate between possible extended gauge models, these processes can measure the amount of Z - Z' mixing, the generation dependence of the Z_2 couplings, and the properties of the new generator associated with the Z_2 . In particular, if the Z_2 arises from a more "conventional" grand unified theory and Z - Z' mixing is absent, the predictions for the three-body decays lie on a straight line in the $r_{l\nu W} - r_{\nu\nu Z}$ plane, with the slope of the line being determined by the mass of the Z_2 . If any of the conditions stated in Eq. (12) are violated, then the values of

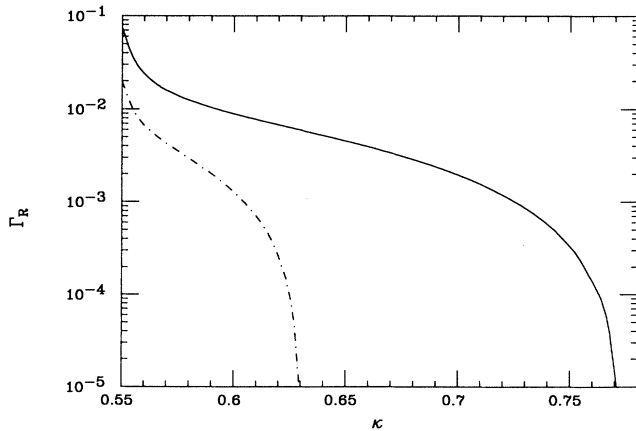


FIG. 9. The reduced width Γ_R for the same cases displayed in Fig. 8.

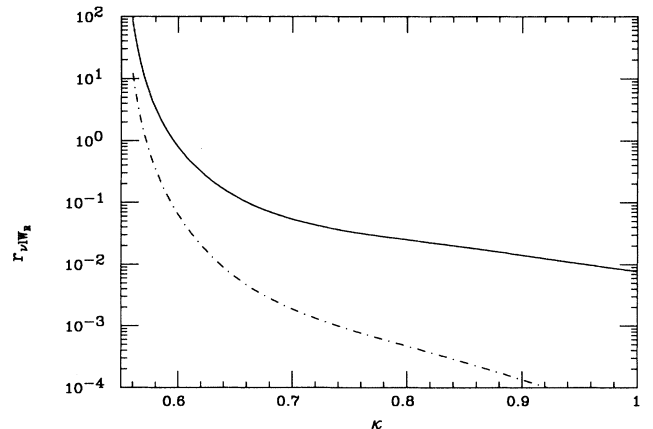


FIG. 10. The ratio $r_{l\nu W_R}$ for the same Higgs representations as shown in Fig. 8.

these decay rates will not lie on this line. The effect of Z - Z' mixing is to increase the rate for $r_{l\nu W}$, while keeping the prediction for $r_{\nu\nu Z}$ relatively unchanged. Hence, a measurement of $r_{\nu\nu Z} > \frac{1}{2}K_Z$ is a definite signal for the violation of conditions (ii) and (iii) of Eq. (12), while a measurement of $r_{l\nu W} > \frac{1}{2}K_W$ could also be a signature for nonzero Z - Z' mixing. Unfortunately, we also found that the rate for the SM background, $pp \rightarrow ZZ \rightarrow Z\nu\bar{\nu}$, eclipses that of $pp \rightarrow Z_2 \rightarrow Z\nu\bar{\nu}$, making detection of this decay appear hopeless, unless the background can be measured directly. Previous analyses have shown [23] that with efficient cuts the process $pp \rightarrow Z_2 \rightarrow Wl\nu$ is observable, and hence is the most useful probe of new gauge boson couplings via three-body decays.

We also find that the decays into a new heavy charged gauge boson, $Z_2 \rightarrow W_2^\pm l^\mp \nu$, can occur in some models at observable rates and would yield even more information on the origin of the extended gauge sector.

We urge our experimental colleagues to consider these promising three-body decays.

Note added. During the preparation of this manuscript we received the related papers in Ref. [23].

This research was supported by the U.S. Department of Energy under Contract No. W-31-109-ENG-38. The research of J.L.H. was also supported in part by the Texas National Research Laboratory Commission.

-
- [1] See, for example, J. L. Hewett and T. G. Rizzo, in *High Energy Physics in the 1990's*, Proceedings of the Snowmass Summer Study, Snowmass, Colorado, 1988, edited by S. Jensen (World Scientific, Singapore, 1989); V. Barger, J. Ohnemus, and R. J. N. Phillips, Phys. Rev. D **35**, 166 (1987); L. S. Durkin and P. Langacker, Phys. Lett. **166B**, 436 (1986); F. Del Aguila, M. Quiros, and F. Zwirner, Nucl. Phys. **B287**, 419 (1987); **B284**, 530 (1987); P. Chiappetta *et al.*, in *Proceedings of the ECFA Large Hadron Collider Workshop*, Aachen, Germany, 1990, edited by G. Jarlskog and D. Rein (CERN Report No. 90-10, Geneva, Switzerland, 1990).
- [2] SDC Collaboration, E. Berger *et al.*, Letter of Intent, SDC Report No. SDC-90-00151, 1990 (unpublished); I. Hinchliffe, M. Mangano, and M. Shapiro, SDC Report No. SDC-90-00036, 1990 (unpublished); I. Hinchliffe, SDC Report No. SDC-90-00100, 1990 (unpublished); I. Hinchliffe, M. Shapiro, and J. L. Siegrist, SDC Report No. SDC-90-00115, 1990 (unpublished); G. Eppley and H. E. Miettinen, SDC Reports Nos. SDC-90-00125, 1990 and SDC-91-00009, 1991 (unpublished); R. Steiner *et al.*, GEM Letter of Intent, 1991 (unpublished).
- [3] J. L. Hewett and T. G. Rizzo, Phys. Rev. D **45**, 161 (1992); see also K. Whisnant, in *Research Directions for the Decade*, Proceedings of the Summer Study on High Energy Physics, Snowmass, Colorado, 1990, edited by E. L. Berger (World Scientific, Singapore, 1991); F. del Aguila and J. Vidal, Int. J. Mod. Phys. A **4**, 4097 (1989); B. Aveda *et al.*, in *Physics of the Superconducting Super Collider, Snowmass, 1986*, Proceedings of the Summer Study, edited by R. Donaldson and J. N. Marx (Division of Particles and Fields of the APS, New York, 1987).
- [4] T. G. Rizzo, Phys. Lett. B **192**, 125 (1987).
- [5] M. Cvetič and P. Langacker, Phys. Rev. D **46**, R14 (1992).
- [6] W. Marciano and D. Wyler, Z. Phys. C **3**, 181 (1979).
- [7] H. Plathow-Besch, in *Proceedings of the Joint International Lepton-Photon Symposium and Europhysics Conference on High Energy Physics*, Geneva, Switzerland, 1991, edited by S. Hegarty, K. Potter, and E. Quercigh (World Scientific, Singapore, 1992).
- [8] J. L. Hewett and T. G. Rizzo, Phys. Rep. **183**, 193 (1989), and references therein.
- [9] For a review and original references, see R. N. Mohapatra, *Unification and Supersymmetry* (Springer, New York, 1986).
- [10] For a related discussion, see M. Cvetič, P. Langacker, and B. Kayser, Phys. Rev. Lett. **68**, 2871 (1992); M. Cvetič and P. Langacker, Phys. Rev. D **42**, 1797 (1990).
- [11] D. Chang, R. Mohapatra, and M. Parida, Phys. Rev. D **30**, 1052 (1984).
- [12] E. Ma, Phys. Rev. D **36**, 274 (1987); Mod. Phys. Lett. A **3**, 319 (1988); K. S. Babu *et al.*, Phys. Rev. D **36**, 878 (1987); V. Barger and K. Whisnant, Int. J. Mod. Phys. A **3**, 879 (1988); J. F. Gunion *et al.*, *ibid.* **2**, 118 (1987); T. G. Rizzo, Phys. Lett. B **206**, 133 (1988).
- [13] R. Foot and O. Hernández, Phys. Rev. D **41**, 2283 (1990); R. Foot, O. Hernández, and T. G. Rizzo, Phys. Lett. B **246**, 183 (1990); **261**, 153 (1991).
- [14] K. T. Mahanthappa and P. K. Mohapatra, Phys. Rev. D **42**, 1732 (1990); **42**, 2400 (1990).
- [15] H. Georgi, E. E. Jenkins, and E. H. Simmons, Phys. Rev. Lett. **62**, 2789 (1989); Nucl. Phys. **B331**, 541 (1990); V. Barger and T. G. Rizzo, Phys. Rev. D **41**, 946 (1990); T. G. Rizzo, Int. J. Mod. Phys. A **7**, 91 (1992).
- [16] See, for example, R. Casalbuoni *et al.*, Phys. Lett. **155B**, 95 (1985); Nucl. Phys. **B310**, 181 (1988); U. Baur *et al.*, Phys. Rev. D **35**, 297 (1987); M. Kuroda *et al.*, Nucl. Phys. **B261**, 432 (1985).
- [17] Such models can occur in some superstring compactification scenarios, S. Samuel (private communication).
- [18] A. Bagnoid, T. K. Kuo, and N. Nakagawa, Int. J. Mod. Phys. A **2**, 1327 (1987); **2**, 1351 (1987).
- [19] X.-G. He *et al.*, Phys. Rev. D **44**, 2118 (1991).
- [20] X. Li and E. Ma, Phys. Rev. Lett. **47**, 1788 (1981); Phys. Rev. D **46**, 1905 (1992); E. Ma, X. Li, and S. F. Tuan, Phys. Rev. Lett. **60**, 495 (1988); E. Ma and D. Ng, Phys. Rev. D **38**, 304 (1988).
- [21] For recent combined analysis of LEP data, see P. Renton, Z. Phys. C **56**, 355 (1992); The LEP Collaborations, CERN Report No. CERN-PPE/91-232, 1991 (unpublished).
- [22] N. Deshpande, J. Gunion, and F. Zwirner, in *Experiments, Detectors, and Experimental Areas for the Supercolider*, Proceedings of the Workshop, Berkeley, California, 1987, edited by R. Donaldson and M. G. D. Gilchriese (World Scientific, Singapore, 1988); N. Deshpande, J. Gri-fols, and A. Mendez, Phys. Lett. B **208**, 141 (1988); F. del Aguila *et al.*, *ibid.* **201**, 375 (1988); **221**, 408 (1989).
- [23] M. Cvetič and P. Langacker, Phys. Rev. D **46**, 4943 (1992); F. del Aguila *et al.*, Phys. Rev. D (to be published).